Arabian Journal of Chemistry (2015) 8, 414–426

King Saud University

Arabian Journal of Chemistry

www.ksu.edu.sa
www.sciencedirect.com

ORIGINAL ARTICLE

Sorption studies of heavy metal ions by salicylic acid–formaldehyde–catechol terpolymeric resin: Isotherm, kinetic and thermodynamics

Riddhish R. Bhatt *, **Bhavna A. Shah** [1]

Department of Chemistry, Veer Narmad South Gujarat University, Udhna Magdalla Road, Surat 395007, Gujarat, India

Received 27 May 2012; accepted 20 March 2013
Available online 28 March 2013

KEYWORDS

Terpolymeric resin;
Ion-exchange;
Sorption;
Thermodynamics;
SEM;
Isotherm

Abstract Terpolymeric resin has been synthesized by condensing salicylic acid with catechol employing formaldehyde as a cross linking agent at 80 ± 5 °C using DMF as a solvent. The resin was characterized by elemental analysis, FTIR, XRD and thermal analysis (TGA, DTA and DTG). The morphology of the resin was studied by optical photographs and scanning electron micrographs (SEM) at different magnifications. The physico-chemical properties have been studied. The uptake behavior of various metal ions viz. Ni(II), Cu(II), Zn(II), Cd(II) and Pb(II) towards synthesized resin has been studied depending on contact time, pH and temperature. The selectivity order found is: Cu(II) > Zn(II) > Pb(II) > Ni(II) > Cd(II). The sorption data obtained at optimized conditions were analyzed by six two parameter isotherm models like Langmuir, Freundlich, Temkin, Dubinin–Radushkevich (D–R), Halsey and Harkins–Jura. The Langmuir, Freundlich and Dubinin–Radushkevich (D–R) isotherms were found better to describe the sorption data with high correlation for the adsorption with a low SSE value for all the metals under study. The adsorption capacities of the SFC resin for removal of Ni(II), Cu(II), Zn(II), Cd(II) and Pb(II) were determined with the Langmuir equation and found to be 0.815, 1.104, 1.215, 0.498, and 0.931 mmol/g respectively. The adsorption process follows first order kinetics and specific rate constant K_r was obtained by the application of Lagergren equation. Thermodynamic parameters viz. ΔG^{ads}, ΔS^{ads} and ΔH^{ads} have also been calculated for the metal-resin systems. The external diffusion rate constant (K_s) and intra-particle diffusion rate

---

* Corresponding author. Mobile: +91 9825901109.
E-mail addresses: rrbhatt_chem@yahoo.com (R.R. Bhatt), bashah@hotmail.com (B.A. Shah).

[1] Mobile: +91 98255 46120.

Peer review under responsibility of King Saud University.

Production and hosting by Elsevier

http://dx.doi.org/10.1016/j.arabjc.2013.03.012

constant (K_{id}) were calculated by Spahn–Schlunder and Weber–Morris models respectively. Desorption studies were done using various desorbing agents viz. de-ionized water, boiled water, various concentrations of HCl, ammonia, thiourea, citric acid and tartaric acid.

1. Introduction

Removing pollutants from wastewater is an important process and is becoming more important with increasing industrial activities. There are many incidents of extensive mortality and/or contamination of fish and other aquatic species from the discharge of heavy metal containing wastewater. The cumulative absorption of small quantities of lead into the human life causes gastrointestinal, genitourinary, musculoskeletal, hematopoetic and reproductive abnormalities and anaemia. Ingestion of large doses of zinc produces toxic symptoms viz. fever, diarrhoea and gastrointestinal tract irritation in humans. Human intact of excessively large doses of copper and nickel leads to severe mucosal irritation and corrosion, widespread capillary damage, hepatic and renal damage and central nervous system irritation followed by depression (Pehlivan and Altum, 2006).

For the removal, separation and enrichment of trace metals from aqueous solutions many techniques are available such as chemical precipitation, oxidation, reduction, coagulation, adsorption, solvent extraction and ion-exchange. The extraction of metal ions using chelating ion exchange resin is a green analytical method since it does not involve the use of toxic chlorinated organic solvents, which are very frequently used in conventional liquid–liquid extraction technique or other methods (Sharma, 2001). Ion exchange is a popular method owing to its applicability to both pre-concentration and separation. The interest in this type of chelating resins is due to the rapid adsorption of metal ions, higher selectivity and less swelling in comparison to the analogous organic polymers (Liu et al., 2011).

Terpolymer resins of o-cresol-urea–formaldehyde have been prepared in the presence of acid catalyst with different molar proportions of monomers (Karunakaran and Magesh, 2011). p-Hydroxybenzoic acid has been used extensively as an analytical reagent in the determination of metal ions due to its chelating property. The synthesis of chelating resin containing p-hydroxybenzoic acid functionality is due to the preparation of insoluble functionalized polymers which can provide more flexible working conditions together with good stability and high capacity for certain metal ions. The ion-exchange resin from p-hydroxybenzoic acid, resorcinol and formaldehyde was derived and studied its ion exchange capacity and selectivity towards Ni(II), Cu(II), Zn(II), Cd(II), and Pb(II) ions (Bhatt et al., 2012). Iminodiacetic acid (IDA) containing commercial resins Amberlite IRC 748 (Zainol and Nicol, 2009) and Amberlite XAD-4 (Hosseini et al., 2006) were employed for the separation and preconcentration of transition metal ions. Some natural porous materials such as diatomite (Sheng et al., 2009) and bentonite (Yang et al., 2009) were also studied for their ion exchange properties.

The terpolymeric resin of 4-hydroxyacetophenone-oxamide-formaldehyde has been synthesized in acidic media (Gurnule et al., 2003). The chelation behavior of the phenolic-formaldehyde polymers towards the trivalent lanthanide metal ions such as La^{3+}, Nd^{3+}, Sm^{3+}, Gd^{3+}, and Tb^{3+} by a static batch equilibrium technique at 25 °C as a function of contact time, pH and concentration (Mubarak et al., 2004). Ion-exchange resins from the diazonium salt of aniline with phenol/resorcinol coupled with formaldehyde have been prepared alkaline medium and studied the uptake behavior of alkali and alkaline earth metal ions. The optimum conditions for effective separation of Cu^{2+} from UO_2^{2+} were also determined (Samal et al., 2000).

Resorcinol–formaldehyde resin has been evaluated for caesium removal and caesium elution characteristics (Burgeson et al., 2006). A new spherical form of resorcinol–formaldehyde resin was also tested for the efficiency of caesium removal from the complex mixture of radioisotopic liquid wastes (King et al., 2006). Resin from salicylic acid and formaldehyde with resorcinol in DMF media has also been prepared and studied for its chelation ion-exchange properties (Shah et al., 2007). Chelating ion-exchange resin from anthranilic acid and formaldehyde with resorcinol in DMF media has been synthesized and applied for the separation of transition and post transition metal ions from synthetic binary mixtures using tartaric acid as eluting agent (Shah et al., 2006). So far no resin based on salicylic acid–formaldehyde–catechol in DMF media has been reported. As industrial effluents are often rich in transition and post transition metal ions, removal and recovery of these metals is an important task for industries.

2. Experimental procedure

2.1. Materials and reagents

Analytical grade chemicals such as salicylic acid, formaldehyde (37%) and catechol were purchased from Qualigens fine chemicals, Mumbai and used as received without further purification. Solutions of acids and alkalies were prepared by dissolving appropriate amount of the particular compound in double distilled water and standardized by the literature methods (Vogel, 1989). Stock solutions of metal salts under study were prepared by dissolving appropriate amount of analytical reagent grade metal acetates in double distilled water. The stock solutions were further diluted with double distilled water to desire concentration for obtaining test solutions. Glassware were cleaned by overnight soaking in chromic acid followed by multiple rinsing with water. All the other reagents used were of analytical grade and were used as such. Double distilled and deionized water was used throughout the research work. All pH measurements were carried out with digital pH meter (Elico CL-44) equipped with a combined glass/calomel electrode. A Perkin-Elmer Model 5000 atomic absorption spectrometer (Perkin-Elmer, Shelton, CT-USA) fitted with nickel, copper, zinc, cadmium and lead hollow cathode lamps was used to analyze the concentration of these heavy metals under study. Three standard solutions with concentration of heavy metal ions in the linear range of the instrument were used to construct calibration curves for each metal ion. During analysis of metal ion concentration, those samples in which the concentration of heavy metal ion is observed beyond the linear range of the references were diluted to appropriate concentrations. All the measurements were repeated three times and those results in which standard deviations were found greater than 0.01 mg/L were not accepted.

2.2. *Resin synthesis*

The resin synthesis was carried out according to the procedure mentioned elsewhere (Shah et al., 2007). Salicylic acid (13.5 g, 0.1 mol) was taken in a 250 ml round bottomed flask and dissolved in DMF solvent (20 ml) to give clear solution. A solution of catechol (11 g, 0.1 mol) in 10 ml DMF was added to the above solution and stirred for two hours. Formaldehyde (0.3 mol as 37%) was added and stirred for an hour. Then the mixture was refluxed on a water bath at 80 ± 5 °C for 2–3 h with constant stirring during which the mixture gelled to a soft mass, which was dark brown in color. A gel was separated from the reaction vessel and cured in an oven at 80–90 °C for 12 h. As carboxylic acid group normally get decomposed above 100 °C, the resin was cured below 90 °C (Shah et al., 2007). The resulting resin was washed with DMF to remove monomer impurities and finally with deionized water. After complete washing cycle, the yield of the resin was found to be 72% (13.7 g). This purified and dry resin sample was finely ground and passed through 20 mesh screen and then 50 mesh screen to get uniform particle size (20–50 mesh). This sieved resin was again washed with water, air dried at room temperature and stored in a polyethylene bottle. The solubility test of resin in different solvents was performed at room temperature and pressure with intermittent shaking. It was found non-melting and insoluble in almost all common organic solvents like acetone, ethanol, benzene, DMF, chloroform etc. and also in acids and alkalies of higher strength (up to 4 M). This sieved resin was characterized using different instrumental techniques and used for all the experiments during the research period.

To convert the resin sample in H^+ form, resin sample having uniform particle size (20–50 mesh) was equilibrated with 1 M HCl solution for 24 h and washed with deionized water till it was free from chloride by testing with silver nitrate solution. This H^+ form of resin was used for further studies. The batch equilibrium method was adopted to study the ion-exchange properties. The physico chemical properties like% moisture content, % solid, apparent density, true density, void volume fraction, sodium exchange capacity were studied according to the literature method (Kunnin, 1958). The results of physico-chemical properties are presented in Table 1.

Table 1 Physico chemical properties of SFC resin.

Properties	Values
% Solid	93.8
True density (g/cm^3)	1.021
Apparent density (g/cm^3)	0.883
Void volume fraction	0.383
Sodium exchange capacity (mmole/g)	3.027
Concentration of fixed ionogenic group	3.473
Particle size (BSS mesh)	20–50
Specific surface area (m^2/g)	183.6
BET surface area (m^2/g)	187.4
Micro pore area (m^2/g)	121.2
Micro pore volume (cm^2/g)	0.0475
Average pore diameter (°A)	0.352
Maximum pore volume (cm^2/g)	0.198

2.3. *Instrumentation*

The particle size distribution was measured by Malvern particle size Analyzer (Mastersizer-2000). The elemental analysis was carried out on a elemental analyser (Carlo Erba-1160). Infra-Red spectra of the synthesized resin sample had been scanned in KBr pallets on FTIR Spectrophotometer (Shimadzu model-8201PC). The powder X-ray diffraction (PXRD) was carried out with advanced diffractometer (Bruker-AXS D8) using monochromatized X-ray beam from nickel filtered Cu Kα (λ = 0.15406 °A) radiation at room temperature. The thermograms (TGA, DTG and DTA) of the SFC resin sample were taken on TG/TGA instrument (Perkin Elmer Pyris Damond) at a constant heating rate of 10 °C/min in N_2 atmosphere at a flow rate of 200 cm^3/min. The surface analysis was done using an optical photograph (Olympus-SZX12) and scanning electron microscope (Philips-XL30) at different magnifications. A temperature controlled water bath shaker (Labline, India) with a temperature variation of ± 1 °C was used for batch sorption studies.

2.3.1. *Nitrogen adsorption/desorption experiments*

For the nitrogen adsorption/desorption experiments SFC-resin was put into the penetrometer and placed into the filling device. Moisture and atmospheric gases were firstly removed from the sample by application of heat and vacuum. Then the temperature was reduced to that of liquid nitrogen and adsorbing gas (nitrogen) was admitted in incremental doses. The surface was determined by applying BET equation, whereas BJH method was used to determine the pore size distribution (Chang et al., 2007).

2.4. *Batch sorption experiments*

Sorption studies were conducted in a routine manner by the batch technique as described earlier (Shah et al., 2007). The effects of important parameters like contact time, pH and temperature were studied. To study the effect of contact time on the sorption of metal ions, H^+ form of accurately weighed (0.250 ± 0.001 g) dry resin samples were taken in different glass stoppered bottles and equilibrated with buffer solutions of desired pH value for 12 h. After decanting buffer solution, 50 ml (0.02 M) metal ion solution of the same pH was added. The amounts of unadsorbed metal ions were determined by means of atomic absorption spectrophotometer at fixed time intervals. To study the effect of pH on the metal ion uptake, it is necessary to buffer the resin and the solutions used. Different sets of accurately weighed (0.250 ± 0.001 g) dry resin having uniform particle size (20–50 mesh) were equilibrated with buffer in different stoppered bottles for 12 h, so that resin attained the desired pH value. After 6 h buffer solutions were decanted and 50 ml of 0.02 M metal ion solutions of varying pH from 3–6 were added. Metal ion solutions were equilibrated at room temperature (30 ± 2 °C) for 12 h with intermittent shaking. After 24 h solutions were filtered with 0.02 μm membrane to separate the resin and solution. The pH of the filtrate was measured and it was found that pH remains stable throughout the experiment (±0.2). From the filtrate unadsorbed metal ions were estimated by means of atomic absorption spectrophotometer. A study on the effect of temperature was performed at a fixed metal ion concentration (0.02 M) for fixed resin loading (0.250 ± 0.001 g) and initial pH (different optimum pH for different metal ions) at four different temperatures i.e. 30, 40, 50, and 60 °C.

The metal concentration retained on the resin (mmol/g) was calculated by using (Eq. (1)).

$$q = \frac{(Co - Ce)V}{M} \times 1000 \tag{1}$$

where, Co and Ce are the initial and equilibrium concentrations (mol/L) of metal ion in solution, V is the volume (L) and W is the weight (g) of the resin.

Each experiment was repeated three times and average values were used in our analysis. If sum of the square error (SSE) was greater than 0.01, the test was repeated to control the error. The standard deviation of the metal uptake per unit weight of resin (S.D.) and sum of the square error (SSE) were calculated using Eq. (2) and Eq. (3) respectively (Oubagaranadin and Murthy, 2009).

$$\text{S.D.}(\%) = \frac{\sum_{i=1}^{N}\left|[(q_{ei})_{cal} - (q_{ei})_{exp}]/(q_{ei})\exp\right|}{N} \times 100 \tag{2}$$

$$\text{SSE} = \sum_{i=1}^{N}(q_{e,cal} - q_{e,exp})^2 \tag{3}$$

where the subscripts "exp" and "cal" show the experimental and calculated values of q_e and N is the number of measurements.

2.5. Desorption and reusability test

For the study of desorption, the SFC loaded with metal ions was placed in various desorption media (de-ionized water, boiled water, various concentrations HCl, ammonia, thiourea, citric acid and tartaric acid) and stirred at 150 rpm for 4 h at room temperature (30 ± 1 °C). After the desorption metal loaded SFC resin was washed to remove unadsorbed metal ion. The final concentration of the metal ion in the aqueous phase was determined by means of atomic absorption spectrophotometer. In order to determine the reusability of adsorbent consecutive adsorption–desorption cycles were repeated five times. After each cycle of adsorption–desorption experiment, SFC resin was washed with 1 M HCl solution and reconditioned for adsorption in the succeeding cycle.

3. Results and discussion

3.1. Characterization of SFC resin

The %C, %H and %O were calculated from the general formula ($C_{14}H_{11}O_7$) of the repeating unit of the assumed structure (scheme-I) of the resin. The values obtain theoretically (practically) are 65.11% (64.85%) and 3.87% (4.18%) for %C and %H respectively. The results of the elemental analysis are in good agreement with calculated values of %C and %H. The values of elemental analysis confirm the proposed structure of the resin presented in the reaction scheme (Fig. 1). The higher degree of agreement of results of elemental analysis and higher yield (72%) indicate the good purity of the synthesized material.

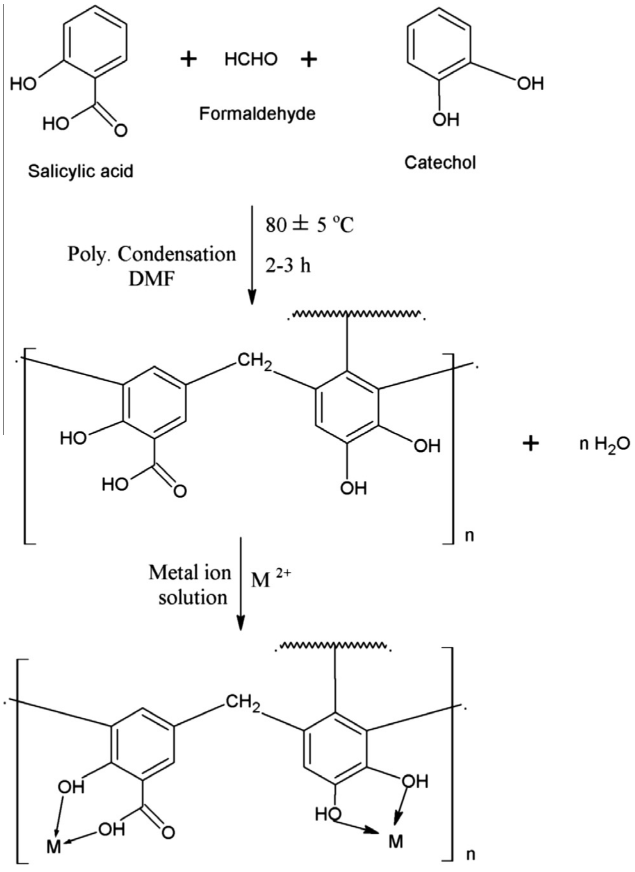

Figure 1 Reaction scheme of synthesis of SFC resin.

The FTIR spectrum of SFC resin is exhibited in Fig. 2. The strong band at 3449.9 cm^{-1} is due to the υ(O–H) stretching of the phenolic group. The presence of medium band at 2920.9 cm^{-1} is due to the υ(C–H) stretching of the methylene group (Shah et al., 2006). The strong medium band at 1630 cm^{-1} can be assigned to υ(C=O) stretching of the aromatic acid group. The weak band at 1462 cm^{-1} is due to δ(C–H) deformation of the methylene group (Silverstain and Bassler, 1991). The weak medium band at 1384.2 cm^{-1} can be assigned to δ(C–O–H) bending of aromatic –OH group. The medium band at 762 cm^{-1} is due to the δ(C–H) bending of the 1,2,3,4-tetra substituted benzene ring (Tager, 1978). The medium band at 667.8 cm^{-1} is due to the δ(C–H) bending of poly ethylene $-(CH_2)^-$ bridges (Shah et al., 2007).

The XRD pattern of SFC is shown in Fig. 3. The XRD pattern of the compound provides information weather the compound is crystalline or amorphous or crystalline and amorphous region co-exist in the same compound (Tager, 1978). No sharp peaks are observed in the diffractogram of the resin. The SFC resin exhibits irregular pattern, which is a characteristic of the amorphous compound (Tager, 1978; Baraka et al., 2007). P-hydroxybenzoic acid–formaldehyde–

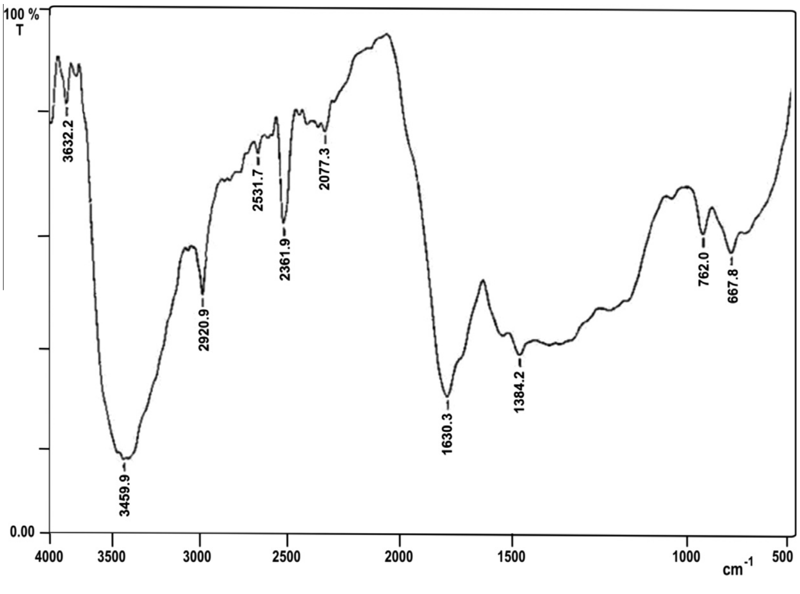

Figure 2 FTIR spectrum of SFC resin.

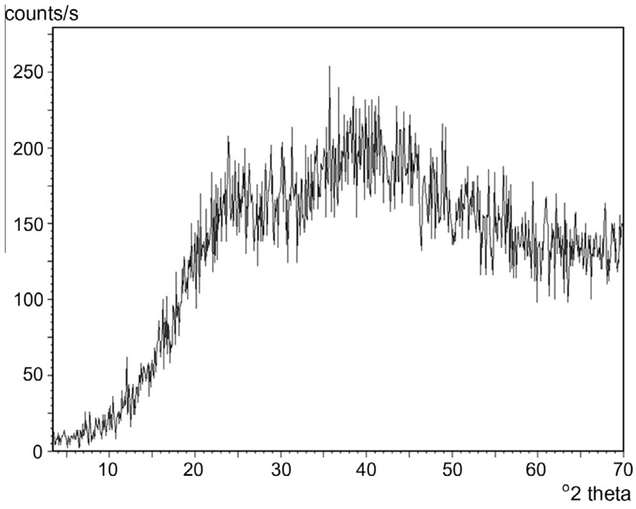

Figure 3 XRD pattern of SFC resin.

resorcinol resin (Bhatt et al., 2012) also exhibited similar XRD pattern, which confirms the amorphous nature of the SFC resin.

3.2. Thermal analysis (TGA, DTA, DTG)

The examination of the result of the thermograms (TGA, DTG and DTA) reveals that SFC resin undergoes degradation in two steps like salicylic acid–formaldehyde–resorcinol resin (Shah et al., 2007). In the beginning of TGA curve, weight loss of 15.1% was observed at 51–150 °C, this may be due to the loss of surface water which is loosely bound and evolved slowly. The maximum rate of weight loss was at 76 °C, which is observed in DTG curve. This is further confirmed from the DTA curve, which shows endothermic moisture loss at 79 °C. The degradation SFC between 210 and 380 °C is expected to be the decomposition of $-CH_2$ group with the weight loss of 14% mass. The second step decomposition of polymeric material starts at 790 °C which extends up to 900 °C involving 13% weight loss. The DTG curve reveals that at 830 °C temperature the rate of weight is the highest. The first step DTA curve of SFC exhibits broad endotherm at 79 °C with enthalpy 269 mJ/mg while in second step the exothermic peak observed at 831 °C with enthalpy −314 mJ/mg. The thermal degradation of the resin may be due to the random cleavage of polymeric resin affording simpler degradation products. Similar observations were reported for salicylic acid–formaldehyde–resorcinol resin (Shah et al., 2007) and anthranilic acid–formaldehyde–resorcinol resin (Shah et al., 2006).

The thermogravimetric analysis has proved to be a useful analytical technique in evaluating kinetic parameters such as order of reaction (n), pre-exponential factor (A), energy of activation (E*), enthalpy of activation (H*), entropy of activation (S*) and free energy of activation (G*), which provides valuable quantitative information regarding the stability of the material. Various methods have been proposed by various investigators to estimate the kinetic parameters of thermal degradation reaction. In the present paper, we have employed Horowitz–Metzger method (Horowitz and Metzger, 1963) and Coats–Redfern methods (Coats and Redfern, 1964) for the estimation of various kinetic parameters of thermal degradation. From the Horowitz–Metzger equation $C_s = (n)^{1/(1-n)}$, where C_s is the mass fraction of the substance (at the DTG peak temperature T_p) and is given by,

$$C_s = W_s - W_f/W_o - W_f \tag{4}$$

Here, W_s stands for the mass remaining at a given temperature T_s, i.e. the DTG peak temperature, W_o and W_f are initial and final masses of the substance respectively. From the Eq. (4) the value of C_s was calculated and was found to be 0.357, which indicates that the decomposition follows the first order kinetics (Horowitz and Metzger, 1963).

The value of energy of activation (Ea) of the thermal degradation of the SFC resin was evaluated from the slope of the least square plots of the relevant data. Pre-exponential factor (A) has been calculated using two different methods viz.

Table 2 Kinetic data of the thermal decomposition of SFC resin at a heating rate of 10 °C/min. in N_2 atmosphere.

Step	T_{range} °C	T_{peak} °C	T_{peak} (°C) [enthalpy (mJ/mg)]	Nature of peak	Parameters	Horowitz–Metzger method	Coats–Redfern method
	TG	DTG	DTA	DTA			
I	51–150	76	79 (269)	Endothermic	E* (kJ mol^{-1})	20.72	22.14
					n	1	1
					A (s^{-1})	1.18×10^7	1.34×10^7
					S* (J K^{-1} mol^{-1})	−110.8	−109.76
					G* (kJ mol^{-1})	56.71	57.76
					H* (kJ mol^{-1})	17.81	19.22
II	790–900	830	831 (−314)	Exothermic	E* (kJ mol^{-1})	74.12	71.81
					n	1	1
					A (s^{-1})	1.62×10^8	1.50×10^8
					S* (J K^{-1} mol^{-1})	−34.84	−30.25
					G* (kJ mol^{-1})	113.84	106.33
					H* (kJ mol^{-1})	75.05	67.70

Horowitz–Metzger and Coats–Redfern. To calculate the entropy of activation, enthalpy of activation, and free energy of activation following equations were employed (Shah et al., 2008).

$$S^* = 2.303\left(\log \frac{Ah}{kT}\right)R \tag{5}$$

$$H^* = E^* - RT \tag{6}$$

$$G^* = H^* - TS^* \tag{7}$$

where, h and k are Plank's and Boltzmann's constants respectively. The negative value of entropy of activation (S_*) indicates the less randomness in the polymeric structure i.e. resin having more regular polymeric backbone. The positive value of enthalpy of activation (H_*) explains that the decomposition process is exothermic. The value of free energy of activation (G_*) was found positive, which indicates that decomposition reaction is slower one (Shah et al., 2008). The values of kinetic parameters calculated by both the methods employed in present communication are in good agreement with each other, which is shown in Table 2.

3.3. Surface analysis (optical and SEM photographs)

Surface analysis has been found to be of great use in understanding the surface features of the material. The morphology of the SFC resin was investigated by optical photographs and scanning electron micrographs to characterize particle shape, size and surface morphology which are shown in Fig. 4. Several observations were made of the resin before the micrographs (optical and SEM) were taken to ensure that the photographed regions were representative of the overall resin sample (Burgeson et al., 2006). The optical and SEM photographs were taken at different magnifications, here in the pres-

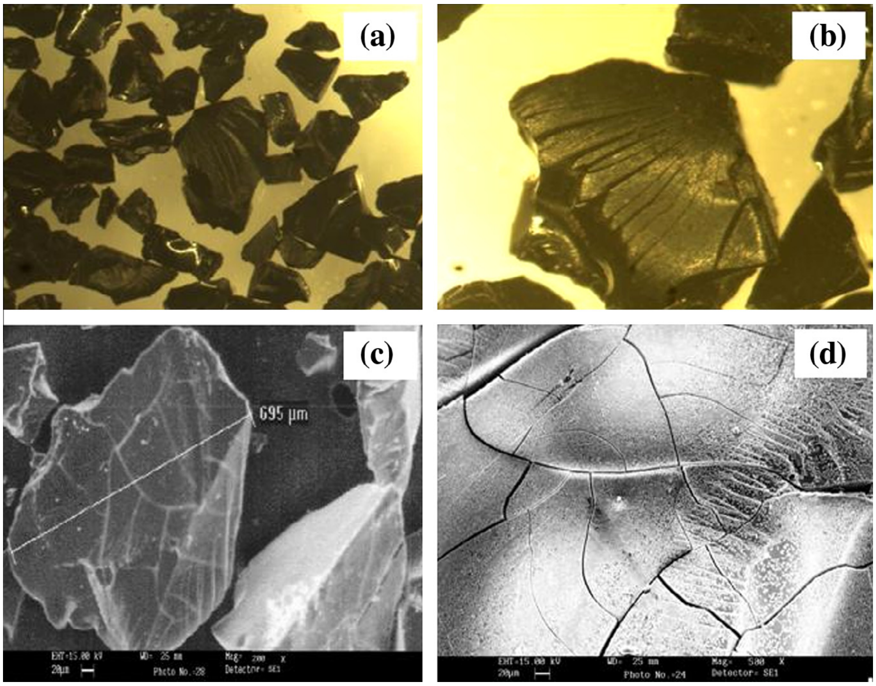

Figure 4 Optical and SEM photograph of SFC resin at different magnifications.

ent communication optical photograph of 90X (Fig. 4a) and 390X (Fig. 4b) magnifications and SEM photograph of 200X (Fig. 4c) and 500X (Fig. 4d) magnifications are presented. Resin appeared dark brown with rough surface in optical photograph. In the SEM photograph of SFC (Fig. 4d) cracks and channels are clearly seen which increases the sorption ability of SFC. Because breaking of large particles tends to open tiny cracks and channels on the particle surface of the material resulting in more accessibility to better diffusion, owing to the smaller particle size (Karthikeyan et al., 2004).

3.4. Effect of contact time and time dependence of the fraction of metal uptake on resin

The exchange of metal ions on resin exhibits the time dependant phenomenon. The rate of exchange for different metal ions is illustrated in Fig. 5. The rate of metal ion adsorption of the resin was determined to ascertain the shortest time period for which equilibrium could be established (Shah et al., 2008). The graph shows that the time required for 50% exchange ($t_{1/2}$) for nickel(II) is 1.5 h, for copper(II) is 50 min., for zinc(II) and lead(II) it is about 55 min. and for cadmium(II) it is 2 h. The faster rate of exchange in the beginning can be explained on the basis of law of mass action (Bhatt et al., 2012). The faster rate of exchange facilitates column chromatographic separation. Kinetics of metal ion exchange mainly depends on the various physical properties like particle size distribution, pore size, physical core structure and diffusion of counter ion (Shah et al., 2007). For 100% uptake of Cu(II) took 8 h, Zn(II) and Pb(II) took 11 h, Ni(II) and Cd(II) took 12 h. So, 12 h is considered as the optimum time for complete equilibration of all the metal ions under study and used for all the further experiments.

Time dependence is determined by plotting the fraction of adsorption, Y_t against the retention time, $t^{1/2}$. The Y_t is defined as below (Eq. (8)):

$$Y_t = C_o - C_t / C_o - C_e \tag{8}$$

where, C_o denotes the initial metal ion concentration, C_t is the concentration of metal ions at time t and C_e is the equilibrium concentration.

The rate of fraction of adsorption Y_t expressed as square root of time is estimated from the three staged curve illustrated in Fig. 6. The initial steep sloped portion is attributed to the transfer of metal ions from the bulk of the solution to the boundary film of the adsorbent and later to its surface. The second stage corresponds to the transfer of the metal ions from the surface to the intraparticular active sites of the resin. This stage is slow and the rate determining step of the reaction. The final stage shows the completion of sorption reaching equilibrium (Bhatt et al., 2012). At equilibrium there is a definite distribution of the solute particle between the solution and the resin particle respectively.

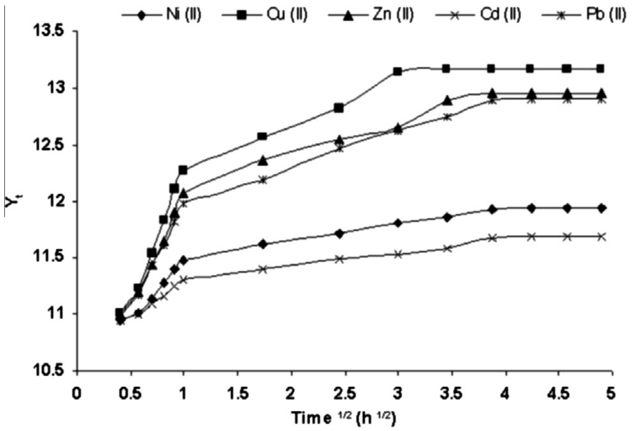

Figure 6 Time dependence of the fraction of adsorption of metal ions on SFC resin.

3.5. Effect of pH

The removal of metal ions from aqueous solution by sorption is highly dependent on pH of the solution that affects the surface charge of the sorbent. Chelating ligand forms complexes with various metal ions at specific pH conditions (Singh and Srivastava, 2006). Therefore, the synthesized resin is used to study the effect of variation in pH on chelating ability of the resin towards various metal ions. The results are presented as exchange capacity against pH for different metal ions in Fig. 7. The results show that adsorption of metal ions was increased with an increase in pH up to a certain value and thereafter decreased. From the nature of the trend observed indicates that the cation exchange behavior of this resin is similar to that of weak acid cation exchangers. In chelating resin sorption capacity is pH dependent. The maximum adsorption

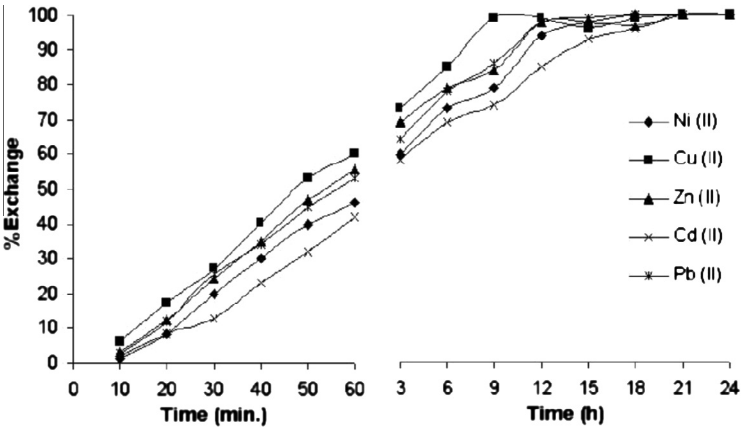

Figure 5 Effect of contact time for metal sorption on SFC resin.

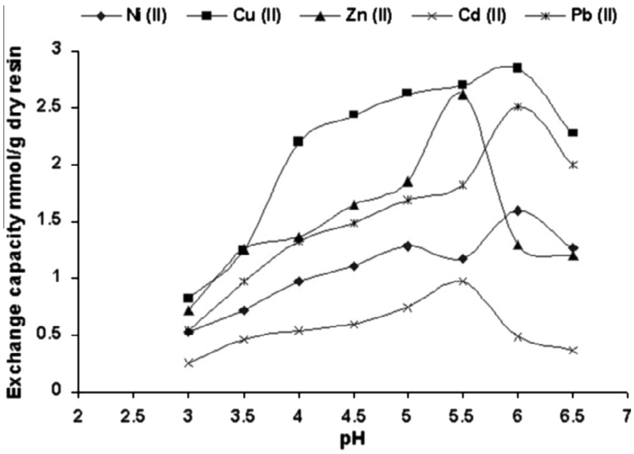

Figure 7 The metal uptake capacity of SFC resin as a function of pH.

for Ni(II), Cu(II) and Pb(II) took place at pH 6, for Zn(II) and Cd(II) it was at pH 5.5. The selectivity order for metal ions is Cu(II) > Zn(II) > Pb(II) > Ni(II) > Cd(II).

An increase in pH increases the negatively charged nature of the sorbent surface. This leads to an increase in the electrostatic attraction between positively charged metal ions and negatively charged sorbent and results in an increase in the adsorption of metal ions. The decrease in the removal of metal ions at a lower pH is due to the higher concentration of H^+ ions present in the reaction mixture which compete with the metal ions for the sorption sites on the sorbent surface. Meanwhile the observed decrease in sorption at higher pH is due to the formation of insoluble hydroxy complexes of the metal ions (Shah et al., 2008). Therefore, pH 6 is considered as the optimum pH for Ni(II), Cu(II) and Pb(II), pH 5.5 is considered as the optimum pH for Zn(II) and Cd(II). The further sorption experiments were carried out at these different optimum pH conditions for different metal ions.

3.6. Effect of temperature and thermodynamic parameters

The effect of temperature on the adsorption of various metal ions on SFC resin was also studied using the optimizing conditions. The temperature was varied from 30 to 60 °C. It was observed that the adsorption of metal ions increases with the increase in temperature (Fig. 8). This is due to the endothermic ion-exchange reaction of divalent cation (Pehlivan and Altum, 2006). The working of an ion-exchange depends on temperature. The surface energy of the SFC resin increases with temperature. Similar results have also been reported earlier for the adsorption of Ni(II), Cu(II), Zn(II),Cd(II) and Pb(II) with commercial resins Dowex 50 (Pehlivan and Altum, 2006) and Amberlite IR 120 (Demirbas et al., 2005).

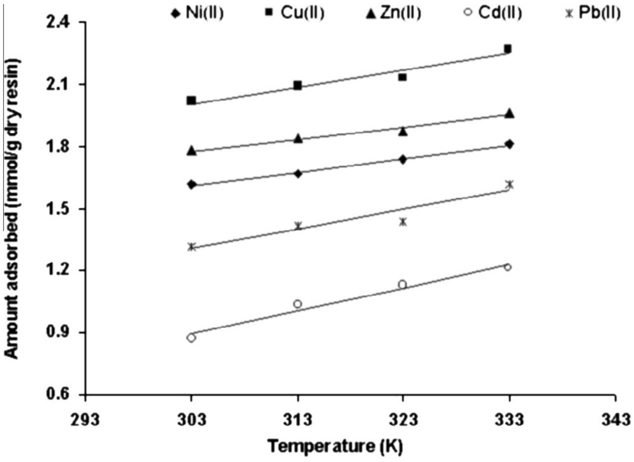

Figure 8 The metal uptake capacity of SFC resin as a function of temperature.

The values of ΔH^{ads}, ΔS^{ads} and ΔG^{ads} were also calculated from the slope and intercept of the Van't Hoff plot of the adsorption of metal ions on SFC resin, i.e. the linear variation of ln K_d with reciprocal temperature $1/T$ (Fig. 9) using the following relation (Eq. (9)):

$$\ln K_d = \frac{\Delta S^{ads}}{R} - \frac{\Delta H^{ads}}{RT} \tag{9}$$

where, K_d is the distribution coefficient (cm^3/g), ΔS^{ads} is the entropy change for the process, and ΔH^{ads} is the enthalpy change for the process. The free energy of the adsorption and ΔG^{ads} was calculated using the following Van't Hoff equation:

$$\Delta G^{ads} = -RT \ln K_d \tag{10}$$

The determination of the thermodynamic parameters for the adsorption of various metal ions on SFC resin is given in Table 3. The value of ΔH^{ads} is negative which indicates an exothermic adsorption process and it indicates that the chelation mechanism dominates (Lima and Airoldi, 2004). The entropy (ΔS^{ads}) is positive corresponding to an increase in degree of freedom of the system due to release of two hydrogen ions for the divalent metal ions under study (Baraka et al., 2007). The negative values of ΔG^{ads} indicate the feasibility of the process and also the spontaneity of the adsorption process. The amount of metal ions adsorbed at equilibrium must increase with increasing temperatures, because ΔG^{ads} decreases with the rise in temperature of the solution (Karthikeyan et al., 2004).

3.7. Kinetic model (Lagergren equation)

It is well established fact that the ion-exchange phenomenon follows reversible first order kinetics, when a single species is

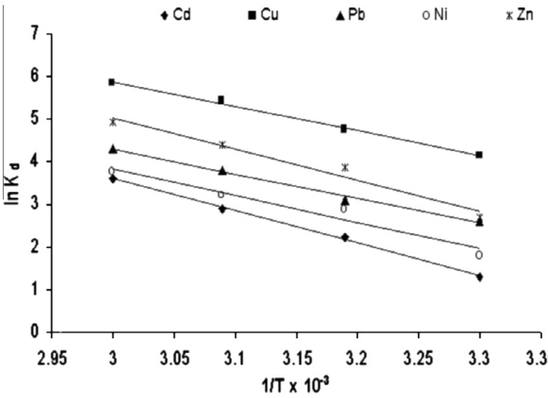

Figure 9 Van't Hoff plot for the adsorption of metal ions on SFC resin.

Table 3 Thermodynamic parameters for metal ion adsorption on SFC resin.

Metal ions	T (K)	$1/T$ (K^{-1})	K_d	ln K_d	ΔG^o (kJ $mol^{-1)}$	ΔH^o (kJ mol^{-1})	ΔS^o (J K^{-1} mol^{-1})
Ni(II)	293	3.30×10^{-3}	7.12	1.9629	−4.7816	−5.153	15.25
	303	3.19×10^{-3}	7.56	2.022	−5.0937		
	313	3.09×10^{-3}	7.73	2.0451	−5.3112		
	323	3.00×10^{-3}	8.02	2.0711	−5.4916		
Cu(II)	293	3.30×10^{-3}	9.44	2.2449	−5.4685	−6.822	19.52
	303	3.19×10^{-3}	9.76	2.2782	−5.7391		
	313	3.09×10^{-3}	10.37	2.3389	−6.0851		
	323	3.00×10^{-3}	10.71	2.3711	−6.3674		
Zn(II)	293	3.30×10^{-3}	7.92	2.0693	−5.0408	−6.141	17.13
	303	3.19×10^{-3}	8.12	2.0943	−5.2758		
	313	3.09×10^{-3}	8.41	2.1294	−5.5412		
	323	3.00×10^{-3}	8.67	2.1598	−5.7999		
Cd(II)	293	3.30×10^{-3}	4.39	1.4793	−3.6035	−7.624	14.84
	303	3.19×10^{-3}	4.52	1.5085	−3.8001		
	313	3.09×10^{-3}	4.77	1.5623	−4.0655		
	323	3.00×10^{-3}	4.91	1.5912	−4.2730		
Pb(II)	293	3.30×10^{-3}	5.19	1.6467	−4.0113	−5.781	18.65
	303	3.19×10^{-3}	5.32	1.6714	−4.2104		
	313	3.09×10^{-3}	5.49	1.7029	−4.4341		
	323	3.00×10^{-3}	5.69	1.7387	−4.6691		

considered on a heterogenous surface (Pehlivan and Altum, 2006). The specific rate constant K_r for the sorbent was determined by Lagergren equation.

$$\log(q_e - q) = \log q_e - (K_r \times t)/2.303 \tag{11}$$

where q_e and q (mmol/g) are the amounts of metal ions adsorbed at equilibrium and time, t (min) respectively. The straight line plot (Fig. 10) of the log (q_e−q) versus time, t (at 30 ± 2 °C) indicates the validity of the Langergran equation for the system and explains that process follows first order kinetics. The values of K_r were calculated from the slop of the plot (Fig. 10) and found to be 9.123×10^{-3}, 14.315×10^{-3}, 13.217×10^{-3}, 6.831×10^{-3}, and $10.185 \times 10^{-3}\ \text{min}^{-1}$ for Ni(II), Cu(II), Zn(II), Cd(II) and Pb(II) respectively. Similar trend in K_r values was reported for Cu^{2+} ($11.3 \times 10^{-3}\ \text{min}^{-1}$) and Ni^{2+} ($9.9 \times 10^{-3}\ \text{min}^{-1}$) with synthetic resin methacrylic acid-co-ethyleneglycol dimethacrylate (Prasad et al., 2002).

3.8. Diffusion models

Sorption kinetics are mainly controlled by various factors including, (i) Solute transfer from the solution to the boundary film of the particle (bulk diffusion) (ii) diffusion from the film to the surface of the sorbent (external diffusion) (iii) diffusion

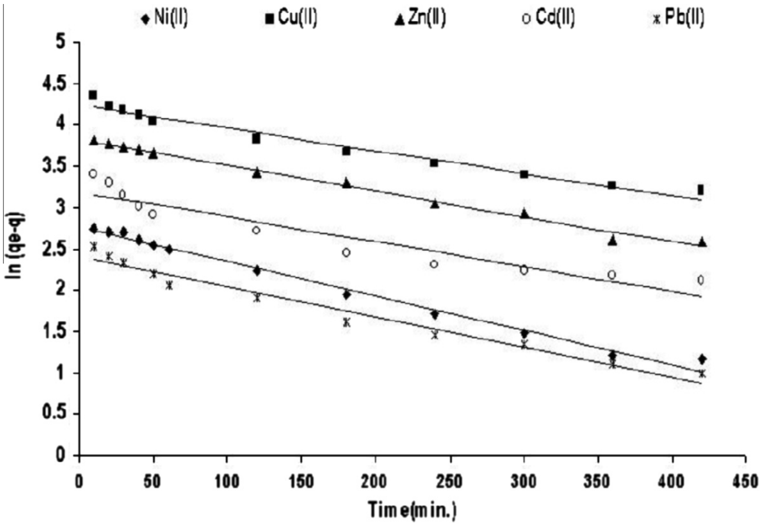

Figure 10 Lagergren plot for specific rate constant of metal ions on SFC resin.

from the surface to the intraparticular sites (intraparticle diffusion) (iv) Solute adsorption by complexation or physico-chemical sorption or ion exchange.

By providing sufficient agitation to avoid particle and solute gradients in the batch reactor makes it possible to ignore bulk diffusion (Prasad et al., 2002). The process of intraparticle diffusion and external diffusion are the rate controlling steps. Several models have been described to discuss the effect of external diffusion and intraparticle diffusion of solute on adsorbent. In the present work Spahn and Schlunder model (Spahn and Schlunder, 1975) and Weber and Morris model (Morris and Weber, 1962) have been chosen to describe the external diffusion and intraparticle diffusion respectively on the resin.

3.8.1. Spahn and Schlunder model

If external diffusion of metal cations (within the diffuse layers outside the sorbent) is the rate limiting step then the sorption data can be fitted into the following relation (Eq. (12)).

$$\ln(C_t/C_o) = -K_s(A/V) \times t \tag{12}$$

where K_s is external diffusion coefficient, C_o is initial metal ion concentration, C_t is concentration at time t, A/V is external sorption area to the total solution volume, and t is sorption time. The external diffusion coefficient can be calculated from the slope of the straight line obtained from the plot of ln (C_t/C_o) versus t (Fig. not shown). The external diffusion model does not show good correlation with the sorption data, because of low correlation coefficients and high SSE values obtained. The external diffusion coefficient (K_s) values of Ni(II), Cu(II), Zn(II), Cd(II) and Pb(II) for SFC were calculated, the values are given in the Table 4. The values for external diffusion coefficient (K_s) for SFC are 0.00167, 0.00523, 0.00334, 0.00125, and 0.00355 mmol/h. Similar type of results has previously been reported while studying uptake behavior of copper and nickel on methacrylic acid-co-ethylene glycol dimethacrylate polymer (Prasad et al., 2002).

3.8.2. Weber and Morris model

An empirically found functional relationship, common to the most sorption processes, is that the uptake varies almost proportionally with $t^{1/2}$, the Weber and Morris plot, rather than with the contact time, t.

$$q_t = k_{id}\, t^{1/2} + I \tag{13}$$

where, q_t is amount of metal ion retained at time t (mmol/g), k_{id} is intra-particle diffusion rate constant, t is the time (h) and I is thickness of the boundary layer. According to the above Eq. (13), a plot of q_t versus $t^{1/2}$ should be a straight line with a slope k_{id} and intercept I when sorption mechanism follows the intraparticle diffusion process. Values of intercept give an idea about the thickness of boundary layer, i.e., larger the intercept the greater is the boundary layer effect (Mall et al., 2005). The values of I for SFC for various metal ions under study are found to be 0.108, 0.211, 0.219, 0.063, and 0.187 mmol/Lh$^{1/2}$ respectively. Weber and Morris pointed out that a functional relation common to the majority of the intraparticle diffusion treatment is that the uptake varies almost proportionately with the half power of the time. The values for intraparticle coefficient (K_{id}) were 0.0366, 0.1162, 0.0778, 0.0310, and 0.0807. From the external diffusion and intraparticle diffusion data, it can be concluded that diffusion process is mainly controlled by intraparticle diffusion with high correlation coefficient value (0.983–0.993) and low SSE value (0.00124–0.00352).

Table 4 Two parameter adsorption isotherm models.

Sr. No.	Two parameter model	Equation
1	Freundlich	$\log q_e = \log k_F + \frac{1}{n}\log C_e$
2	Langmuir	$\frac{C_e}{q_e} = \frac{1}{q_m k_L} + \frac{C_e}{q_m}$
3	Dubinin–Redushkevich	$\ln q_e = \ln q_m - \beta\varepsilon^2$
4	Temkin	$q_e = B_1 \ln k_T + B_1 \ln C_e$
5	Harkins–Jura	$\frac{1}{q_e^2} = [\frac{B}{A}] - [\frac{1}{A}]\log C_e$
6	Halsey	$\ln q_e = [(\frac{1}{n})\ln k] - (\frac{1}{n})\ln C_e$

3.9. Sorption isotherms

The Langmuir, Freundlich, Temkin, Dubinin–Radushkevich, Harkins–Jura and Halsey isotherm parameters were calculated in same way as the related researches did in the literature (Oubagaranadin and Murthy, 2009). The linearized form of Langmuir (1916), Freundlich (1906), Temkin (1940), Dubinin and Radushkevich (1960), Harkins and Jura (1943) and Halsey (1948) adsorption isotherms are given in Table 5. The constant parameters, correlation coefficient (R^2) and SSE value are summarized in Table 6.

A preliminary screening of the corresponding data has shown that Freundlich model with high correlation coefficient value (0.9877–0.9989) and low SSE value (0.00215–0.00785) was found best fit the experimental data. The adsorption capacity (K_f) and the adsorption intensity ($1/n$) are directly obtained from the slope and the intercepts of the linear plot respectively and data are given in Table 6. The determined value of $1/n$ is of the same magnitude as those reported commercial macrorecticular chelating resin Duolite GT-73 (Vaughan et al., 2001). The higher fractional values of $1/n$ signify that strong adsorption forces are operative on the system. The magnitude of $1/n$ also gives indication of the favourability and capacity of the adsorbent/adsorbate system. The value 'n' between 1 and 10 represents favorable adsorption (Stephan and Sulochana, 2002). For all the metal-resin systems reported here, the exponent is $1 < n < 2$ showing beneficial adsorption (Table 6). Freundlich constants K_f were calculated as 35.41, 68.72, 54.70, 21.35, 41.35 and n were calculated as 1.8574, 1.6562, 1.8286, 1.5658, 1.7718 for Ni(II), Cu(II), Zn(II), Cd(II) and Pb(II) respectively.

The Langmuir constants q_{max} and b related to adsorption capacity and energy of adsorption respectively were calculated as same way as the related researches did in the literature (Oubagaranadin and Murthy, 2009). These constant q_{max} were calculated as 0.815, 1.104, 1.215, 0.489, and 0.931 mmol/g as maximum capacity for Ni(II), Cu(II), Zn(II), Cd(II) and Pb(II) respectively. The results were comparable with commercial resin Duolite GT-73 (Vaughan et al., 2001). The q_{max} of Duolite GT-73 for Cu(II), Cd(II) and Pb(II) were 62, 106 and 122 mg/g respectively. Prasad et al. (2002) reported q_{max} values for synthetic resin (methacrylic acid-co-ethyleneglycol dimethacrylate) were 416.67 and 588.24 mg/g for Cu(II) and Ni(II) respectively. Sorption energy constants of SFC for Ni(II), Cu(II), Zn(II), Cd(II) and Pb(II) are 0.0522, 0.0567, 0.0534, 0.0464, and 0.0775 L/mmol respectively. The essential charac-

Table 5 Adsorption isotherm data of various isotherm models.

Parameter	Metal ions				
	Ni(II)	Cu(II)	Zn(II)	Cd(II)	Pb(II)
Langmuir constant					
q_{max} (mmol/L)	0.815	1.104	1.215	0.489	0.931
b (L/mg)	0.0522	0.0567	0.0534	0.0464	0.07753
R_L	0.4852	0.4887	0.4968	0.5279	0.3986
R^2	0.9852	0.9863	0.9871	0.9881	0.9875
SSE	0.01304	0.0304	0.0289	0.0376	0.0541
Freundlich constant					
K_F(mmol/g)(L/g)$^{1/n}$	35.41	68.72	54.70	21.35	41.35
n	1.8574	1.6562	1.8286	1.5658	1.7718
R^2	0.9981	0.9925	0.9938	0.9954	0.9985
SSE	0.00351	0.00124	0.00215	0.00688	0.00785
Temkin constant					
b_T (J/mol)	3.46×10^2	5.13×10^2	6.81×10^2	4.19×10^2	4.51×10^2
k_T (L/mmol)	0.6543	0.6250	0.5864	0.5886	0.9353
R^2	0.9823	0.9845	0.9758	0.9787	0.9874
SSE	0.5462	0.4414	0.2644	0.8929	0.7448
Dubinin–Redushkevich (D–R) constant					
β	1.21×10^{-3}	6.11×10^{-4}	8.74×10^{-4}	3.78×10^{-3}	2.42×10^{-3}
q_m	0.860	1.344	1.025	0.419	0.931
E	15.18	20.70	19.15	14.66	13.48
R^2	0.9886	0.9849	0.98052	0.9829	0.9864
SSE	0.0304	0.0601	0.0618	0.0804	0.0646
Harkins–Jura constant					
A	1.5360	2.3463	1.5639	2.8776	4.7448
B	1.1342	1.5253	1.2888	1.6612	1.8879
R^2	0.8891	0.8563	0.8672	0.8747	0.8925
SSE	0.7886	0.8847	0.7161	0.8650	0.7287
Halsey constant					
n	−1.5874	−1.6458	−1.7286	−1.5128	−1.67084
k	1.0522	1.5757	2.60781	1.42369	1.55499
R^2	0.9012	0.8152	0.9138	0.8854	0.8975
SSE	1.0886	1.1766	0.9441	1.2655	1.1145

Table 6 Data of external and intra-particle diffusion rate constant.

Metal ion	External diffusion			Intra-particle diffusion			
	K_s	R^2	SSE	K_{id}	I	R^2	SSE
Ni(II)	0.00167	0.9172	0.35421	0.0766	0.108	0.993	0.00082
Cu(II)	0.00523	0.9261	0.28712	0.1162	0.211	0.989	0.00152
Zn(II)	0.00334	0.8974	0.34261	0.0778	0.219	0.983	0.00211
Cd(II)	0.00125	0.9138	0.72563	0.0701	0.103	0.992	0.0009
Pb(II)	0.00355	0.8963	0.62524	0.0807	0.187	0.989	0.00324

teristics of Langmuir equation can be expressed in terms of a dimensionless separation factor or equilibrium parameter, R_L (Singh and Srivastava, 2001). The values indicate the isotherm to be either unfavorable ($R_L < 1$), linear ($R_L = 1$), favorable ($0 < R_L < 1$) or irreversible ($R_L = 0$). The values of R_L obtained for the metal-resin system are shown in Table 6. The R_L values for all the metals under study lying between 0 and 1 indicate favorable adsorption (Karthikeyan et al., 2004).

For Temkin isotherm it was found that the values of R^2 for all the adsorbents under study are slightly lower than Langmuir values. Therefore it was also considered that the adsorption of metals under study on SFC resin also follow the Temkin isotherm closely. From the values of the Temkin isotherm constant b_T, it can be observed that the heat of adsorption is maximum for SFC-Cd(II) system, whereas it is the lowest for SFC-Cu(II) system.

In order to study the nature of the adsorption phenomenon, physical sorption or chemical sorption, the data were applied to Dubinin–Radushkevich (D–R) isotherm model. The D–R equations are as follows (Eqs. (14)–(17)):

$$q_e = q_m \exp(-\beta\varepsilon^2) \quad (14)$$

where q_e is the amount of metal adsorbed on SFC resin (mmol/g), q_m is the maximum amount of metal ions that can be adsorbed on SFC under the optimized experimental conditions (mmol/g), β is a constant related to sorption energy ($\text{kJ}^2\,\text{mol}^{-1}$) and ε is Polanyi potential which is mathematically represented as:

$$\varepsilon = RT\ln(1 + 1/C_e) \tag{15}$$

where, R is the gas constant in $\text{kJ mol}^{-1}\,\text{K}^{-1}$, T is the absolute temperature in Kelvin and C_e is the equilibrium concentration of metal ion in solution (mmol/g). The linearized form of the D–R isotherm is:

$$\ln q_e = \ln q_m - \beta\varepsilon^2 \tag{16}$$

where, $\ln q_e$ was plotted against ε^2, straight lines were observed for all the metal ions (Fig. not shown). The values of β and q_m were computed from the slope and intercept of these straight lines. The values of β obtained were 1.217×10^{-3}, 6.109×10^{-4}, 8.744×10^{-4}, 3.781×10^{-3}, and 2.423×10^{-3} for Ni(II), Cu(II), Zn(II), Cd(II) and Pb(II) respectively. The values of C_m were 86.90, 134.04, 102.15, 41.89, and 93.51 mg/g respectively. The value of sorption energy "E" can be correlated to β by using the following relationship.

$$E = \frac{1}{\sqrt{-2\beta}} \tag{17}$$

This is the free energy of transfer of one mole of solute from infinity to the surface of SFC resin. This parameter gives information whether adsorption mechanism is ion-exchange or physical sorption. If the magnitude of E is between 8 and 16 kJ mol^{-1} the adsorption process follows by ion-exchange, while value of $E < 8\ \text{kJ mol}^{-1}$ the adsorption process is of a physical nature (Ozcan et al., 2005). In the present study the numerical values of E evaluated from Eq. (17) are 15.18, 20.70, 19.15, 11.66, and 13.48 kJ mol^{-1} for Ni(II), Cu(II), Zn(II), Cd(II) and Pb(II) respectively, which is expected for chemisorption based on ion-exchange (Khalid et al., 2007).

The Harkins–Jura and Halsey model explain multilayer adsorption. The Harkins–Jura and Halsey model exhibits a very low R^2 value and a very high SSE value indicates that the adsorption process follows fairly these models.

3.10. Desorption and reusability

The desorption profile is important for the column chromatographic study for the elution of metal ions. Desorption of heavy metal ions from metal loaded SFC resin was studied by the batch method. Various types of desorbing agents such as deionized water, boiled water, various concentrations of HCl, ammonia, thiourea, citric acid and tartaric acid were tested for desorption of adsorbed metal ion loaded SFC resin. Amount desorbed by these desorbing agents was studied and results are mentioned in Table 7. Deionized water, boiled water and ammonia could not desorb heavy metal ions effectively (about 2–6%). In case of HCl, thiourea, citric acid and tartaric acid results indicate that desorption increases with increase in the concentration of desorbing agents. Thiourea removed 61–74% of metal ions from the metal loaded SFC

Table 7 Desorption data of metal ion from loaded SFC resin.

Eluent used	% Desorption of Metal ions from SFC resin				
	Ni(II)	Cu(II)	Zn(II)	Cd(II)	Pb(II)
De-ionized water	2.32	2.56	1.35	4.43	1.54
Boiled water	3.01	2.41	2.03	3.87	1.612
HCl (M)					
0.1	61.412	50.53	56.73	72.45	49.62
0.5	77.62	63.62	60.15	79.42	58.52
1.0	89.25	83.81	80.32	91.82	63.82
1.5	94.98	90.54	94.86	95.70	88.70
Ammonia (M)					
0.1	3.12	1.37	1.47	3.12	2.14
0.5	5.91	4.87	2.76	5.15	2.95
1.0	6.45	5.46	3.80	5.62	3.56
1.5	6.44	5.89	5.10	6.03	5.38
Thiourea (M)					
0.1	61.01	58.14	59.998	65.08	60.98
0.5	68.99	68.99	60.01	68.12	65.12
1.0	71.43	70.83	71.50	75.08	70.08
1.5	73.89	72.19	74.13	76.76	72.76
Citric acid (M)					
0.1	69.88	65.33	59.68	74.77	58.77
0.5	76.43	75.00	62.73	78.85	68.85
1.0	81.35	78.25	79.89	82.25	71.25
1.5	85.98	82.25	79.82	86.95	79.95
Tartaric acid (M)					
0.1	62 .46	63.52	58.24	76.72	58.31
0.5	75.87	74.83	61.36	83.83	67.27
1.0	83.62	75.21	78.34	92.13	67.28
1.5	94.23	82.18	78.41	93.41	78.43

resin. Tartaric acid and citric acid showed approximately equivalent efficiency, for all the metals under study it can desorb the metals in the range of 79–86%. In case of Ni(II) and Cd(II), tartaric acid acts as a better eluent but 100% elution was not possible. Hydrochloric acid due to its highest metal desorption activity (94–98%) was selected as a desorbing agent for further studies on adsorption–desorption cycles of metal to test the reusability of SFC resin. In order to determine the reusability of the resin sorption–desorption cycle was repeated five times in batch experiments. For this purpose hydrochloric acid of different concentrations depending upon the metal ions was used to desorb the sorbed metal ions. The regenerated resin was washed thoroughly with deionized water and converted into H^+ form and used for the next sorption cycle. The result of reusability test demonstrates that even after five adsorption–desorption cycles adsorption capacity was not significantly changed (about 1%). This indicates that the reuse of material is feasible.

4. Conclusions

Thermogravimetric analysis suggests that the decomposition reaction is first order, exothermic and slower one. The resin shows lower percentage of moisture content compared to other reported resins which indicates the high degree of cross-linking in this resin. So, it become less dense and expected to be more porous. The pH titration study of the resin was carried out and results are studied. Resin stability test indicates that SFC is convenient for chromatographic separation as it shows no significant change in its capacity up to five loading acid washing cycles. The adsorption follows both Langmuir and Freundlich isotherm models. The data obtained from Langmuir, Freundlich and D–R equations indicate that beneficial adsorption occurs through monolayer mechanism involving ion-exchange/chelation phenomenon. Thermodynamic parameters show that adsorption process is exothermic and spontaneous. From the results of various diffusion models, it can be concluded that diffusion process is mainly controlled by intra-particle diffusion.

Acknowledgment

The authors are grateful to The Head, Dept. of Chemistry, Veer Narmad South Gujarat University, Surat, for providing laboratory facility.

References

Baraka, A., Hall, P.J., Heslop, M.J., 2007. J. Hazard. Mater. 140, 86–94.

Bhatt, R.R., Shah, B.A., Shah, A.V., 2012. Malays. J. Anal. Sci. 16, 117–133.

Burgeson, I., Cook, B., Blandchard, D., Weier, D., 2006. Sep. Sci. Technol. 41, 2373–2390.

Chang, P., Wang, X., Yu, S., Wu, W., 2007. Colloids Surf. A 302, 75–81.

Coats, A.W., Redfern, J.P., 1964. Nature 201, 68–69.

Demirbas, A., Pehlivan, E., Gode, F., Altun, T., Arslan, G., 2005. J. Colloid Interface Sci. 282, 20–25.

Dubinin, M.M., Radushkevich, B., 1960. Chem. Rev. 60, 235–266.

Freundlich, H.M.F., 1906. Z. Phys. Chem. (Leipzig) 57, 385–470.

Gurnule, W.B., Rahangdale, P.K., Paliwal, L.J., Kharat, R.B., 2003. J. Appl. Polym. Sci. 89, 787–790.

Halsey, G., 1948. J. Chem. Phys. 16, 931–937.

Harkins, W.D., Jura, G., 1943. J. Chem. Phys. 11, 431–432.

Horowitz, H., Metzger, G., 1963. Anal. Chem. 35, 1464–1468.

Hosseini, M.S., Raissi, H., Madarshahian, S., 2006. React. Funct. Polym. 66, 1539–1545.

Karthikeyan, G., Anbalagan, K., Andal, N.M., 2004. J. Chem. Sci. 116, 119–127.

Karunakaran, M., Magesh, C., 2011. Arab. J. Chem. 4, 339–348.

Khalid, N., Ali, S., Pervez, S., 2007. Sep. Sci. Technol. 42, 203–222.

King, W.M., Fondeur, F.F., Wilmarth, W.R., Pettis, M.E., McCollum, S.W., 2006. Sep. Sci. Technol. 41, 2461–2474.

Kunnin, R., 1958. Ion Exchange Resin. Wiley, London.

Langmuir, I., 1916. J. Am. Chem. Soc. 38, 2221–2295.

Lima, I.S., Airoldi, C., 2004. Thermochim. Acta. 421, 133–139.

Liu, F., Li, L., Ling, P., Jing, X., Li, C., Li, A., You, X., 2011. Chem. Eng. J. 173, 106–114.

Mall, I.D., Srivastava, V.C., Agarwal, N., Mishra, I.M., 2005. Colloids Surf. A 264, 17–28.

Morris, J.C., Weber, W.J., 1962. Advance in Water Pollution Research. Pergamon Press, New York.

Mubarak, M., Rimawi, F., Khalili, F., 2004. Solv. Extr. Ion Exch. 22, 721–725.

Oubagaranadin, J.U.K., Murthy, Z.V.P., 2009. Eur. J. Wood Wood Prod. 67, 197–206.

Ozcan, A.S., Erden, B., Ozcan, A., 2005. Colloids Surf. A 266, 73–81.

Pehlivan, E., Altum, T., 2006. J. Hazard. Mater. B134, 149–156.

Prasad, H.H., Popat, K.M., Anand, P.S., 2002. Indian J. Chem. Technol. 9, 385–393.

Samal, S., Das, R., Day, R., 2000. J. Appl. Polym. Sci. 77, 3128–3141.

Shah, B.A., Shah, A.V., Bhandari, B.N., Bhatt, R.R., 2008. J. Iran. Chem. Soc. 5, 252–261.

Shah, B.A., Shah, A.V., Shah, P.M., 2006. Iran. Polym. J. 15, 809–819.

Shah, B.A., Shah, A.V., Bhatt, R.R., 2007. Iran. Polym. J. 16, 173–184.

Sharma, R.K., 2001. Pure Appl. Chem. 73, 181–186.

Sheng, G., Wang, S., Hu, J., Lu, Y., Li, J., Dong, Y., Wang, X., 2009. Colloids Surf. A 339, 159–166.

Silverstain, R.M., Bassler, G.C., 1991. Spectrometric Identification of Organic Compound. John Wiley and Sons Inc., New York.

Singh, D.K., Srivastava, M., 2006. J. Liq. Chromatogr. Related Technol. 29, 1433–1445.

Singh, D.K., Srivastava, B., 2001. Indian J. Chem. Technol. 8, 133–139.

Spahn, H., Schlunder, U., 1975. Chem. Eng. Sci. 30, 529–535.

Stephan, I.B., Sulochana, N., 2002. Indian J. Chem. Technol. 9, 201–205.

Tager, A., 1978. Physical Chemistry of Polymer. Mir Publisher, Moscow.

Vaughan, T., Seo, C.W., Marshall, W.E., 2001. Bioresour. Technol. 78, 133–139.

Vogel, A.I., 1989. Quantitative Inorganic Analysis, Fifth ed. Longaman, London.

Yang, S., Li, J., Lu, Y., Chen, Y., Wang, X., 2009. Appl. Radiat. Isot. 67, 1600–1608.

Zainol, Z., Nicol, M., 2009. Hydrometallurgy 99, 175–180.